ISBN: 978-3-95450-249-3 ISSN: 2673-5350 doi: 10.18429/JACoW-IBIC2024-WEP18

# TROUBLESHOOTING THE IONIZATION PROFILE MONITOR (IPM) FOR CSNS 1.6 GeV RCS*

M. A. Rehman†, R. Yang‡, Z. Xu, W. Huang, X. Nie, X. Li, S. Wang
Institute of High Energy Physics, Chinese Academy of Sciences (CAS), Beijing, China
also at China Neutron Spallation Source, Dongguan, China
P. Forck, GSI Helmholtzzentrum fur Schwerionenforschung GmbH, Darmstadt, Germany
J. Sun, Paul Scherrer Institut, Villigen PSI, Switzerland

*Abstract*

Non-invasive and turn-by-turn beam transverse profile monitoring is essential for the tunning and operating CSNS 1.6 GeV Rapid Cyclic Synchrotron (RCS). A residual gas Ionization Profile Monitor (IPM) was designed and installed in RCS for horizontal beam profile measurement. However, several challenges related to Electromagnetic Interference (EMI), vacuum, and MCP operation in the IPM were identified. The EMI is induced by the beam itself and further accelerator components. An improved Faraday cage was implemented to counteract the EMI issues. In order to achieve the desired MCP gain, a suitable pull-down resistor was incorporated into the MCP power supply circuit. After these improvements, the IPM was commissioned successfully. This paper will describe the challenges of IPM and early beam commissioning results.

## INTRODUCTION

The China Spallation Neutron Source (CSNS) [1, 2] is one of the major scientific facilities in China, constructed to deliver intense pulsed neutron beams for diverse scientific research and industrial applications. The CSNS accelerator complex comprises an injector LINAC that accelerates the $H^-$ beam to 80 MeV. Subsequently, the $H^-$ beam undergoes electron stripping through a foil, leaving behind a proton beam that is then injected into a Rapid Cyclic Synchrotron (RCS) to further increase beam energy to 1.6 GeV. The accelerated proton beam is delivered to a solid Tungsten target to produce neutrons. The parameters of RCS are described in Table 1.

Table 1: CSNS RCS Parameters

| Parameters | Values | Units |
|---|---|---|
| Injection Energy | 80 | MeV |
| Ring Circumference | 227.92 | m |
| Extraction Energy | 1.6 | GeV |
| Repetition Rate | 25 | Hz |
| Number of Bunches | 2 | |
| $f_{rev}$ | 1.02 – 2.44 | MHz |
| Beam Intensity | $2.5 \times 10^{13}$ | ppb |

The non-invasive and turn-by-turn monitoring of the beam transverse profile plays a critical role in the tuning and operation of a high-current accelerator, such as the CSNS RCS. For this purpose, a prototype Ionization Profile Monitor (IPM) system has been developed to measure the horizontal beam profile.

The first IPM was proposed and developed in 1966 [3]. In the IPM, the charged particle beam interacts with the residual gas components in the vacuum duct, leading to the production of secondary ions/electrons. These secondary particles have the same spatial distribution as the primary beam. An external electric field is used to collect the ions/electrons products. Due to the low yield of the secondary particles, an additional detector is necessary. Typically, a Micro Channel Plate (MCP) is used as a pre-amplifier, offering a signal amplification of $10^4$–$10^7$. A simplified illustration of the IPM principle is shown in Fig. 1 (a).

In Fig. 1 (b), the 3D model of the RCS's IPM is displayed. The field cage of the IPM comprises 14 electrodes with an aperture of 220 mm × 231 mm. The MCP [4] is a double-stage with a gain of $10^6$ and consists of 32-strip anode strips, each with a width of 2.4 mm and a mutual spacing of 0.1 mm. The effective area of the MCP is 81 mm × 31 mm.

The readout cables from the MCP are first connected to the Common Mode Choke (CMC) and then connected to the 32-channel digitizer (NI, PXIe-5172). The digitizer has a bandwidth of 100 MHz and a sampling rate of 250 MSa/s. The input impedance of each channel on the digitizer is 50 Ω.

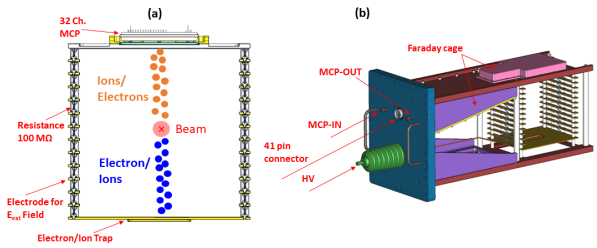


Figure 1: (a) The principle of the IPM. (b) The 3D model of the RCS IPM. The front flange consists of several feedthroughs to apply high voltage to the field cage, MCP and readout signal from the MCP. The MCP and readout cables are enclosed in the Faraday cage.

* Work supported by National Science Foundation for Young Scientists of China (12305166).
† rehman@ihep.ac.cn
‡ yangrenjun@ihep.ac.cn

ISBN: 978-3-95450-249-3 ISSN: 2673-5350 doi: 10.18429/JACoW-IBIC2024-WEP18



## TROUBLESHOOTING THE IPM

Several challenges were encountered during the initial stage of the IPM commissioning. The main challenges are listed below:

- Electro-Magnetic Interference (EMI)
- MCP Operation
- Vacuum Issues
- Analysis Techniques

The details of these challenges and mitigation will be described in the coming sections.

### *Electro-Magnetic Interference (EMI)*

At the early stage of IPM commissioning two kinds of Electro-Magnetic Interference (EMI) have been observed:

- Common Mode Noise
- Beam Induced Noise

The common mode noise occurs when unwanted electrical signals or interference from various accelerator components, such as AC magnets, RF cavities, and ground loops, induce interference on the IPM readout cables. The common mode signal from the accelerator components flows in the same direction on both conductors of the readout coaxial cable, creating a voltage potential between the conductors. This can result in an imbalance in the signal levels between the conductors, leading to interference and distortion in the transmitted signal.

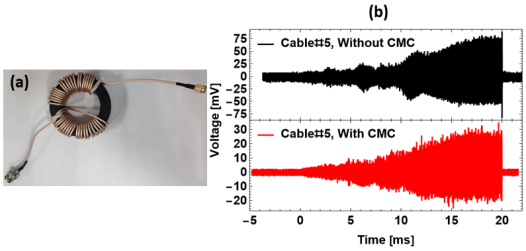


Figure 2: (a) The photo shows the CMC to suppress common noise on the IPM readout cables. (b) The signal is from one of the anode strips of the MCP, with the image current from the beam and accelerator components, common mode noise is evident. The implementation of the CMC effectively suppressed the common mode noise.

The common mode choke (CMC) was utilized to address this issue. It comprises a coaxial cable wound around a single magnetic core. Specifically, 40 turns of RG316 cable are wound around a magnetic core. arranged in a cross configuration. The photo of the CMC is depicted in Fig. 2 (a). When common mode noise passes the choke, the magnetic fields generated by the coils combine, resulting in a high impedance for the common mode signal. This effectively suppresses the common mode noise. In Fig. 2 (b), at the top, the signal from one of the channels of IPM is illustrated. In this particular instance, the IPM was off, but noise was predominant on the readout cable. However, after implementing the CMC, the noise was reduced to half.

The electromagnetic field of the proton beam induces image current on the isolated copper anodes of MCP. The image current is visible in Fig. 2 (b); as the beam energy increases from 80 MeV to 1.6 GeV, the peak image current on the MCP anodes also increases. As depicted in Fig. 2 (b), using CMC suppresses the common mode noise. However, the image current cannot be suppressed. A good electromagnetic shielding of the MCP anode is necessary to prevent this issue. To address this, the following measures were implemented:

- RF shield
- Faraday cage

The Honeycomb structure in front of the MCP is used as an RF shield to prevent induced image current on the anodes. The RF shield is made of stainless steel, coated with nickel, and has a thickness of 6 mm with a hole width of 3.2 mm. It also allows sufficient clearance to pass ionized products without any interference. The shielding effectiveness (SE) of the hexagonal honeycomb can be approximated using the following formula [5]:

$$SE = 17.5\frac{d}{g}\sqrt{1-\left(\frac{gf}{96659}\right)^2}, \quad (1)$$

where $d$ and $g$ represent the thickness and width of the honeycomb, while $f$ denotes the frequency in MHz. The SE is approximately −57 dB within the frequency range of up to 500 MHz. However, it should be noted that the above formula may not provide precise results for the lower megahertz frequency range, and it may be necessary to incorporate higher-order terms or conduct numerical simulations for a more accurate estimation.

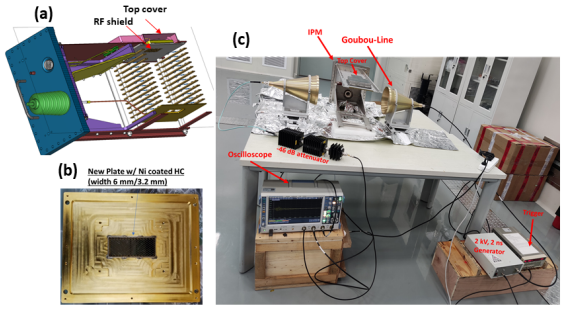


Figure 3: (a) The IPM model shows the location of the RF shield. (b) The Honeycomb (HC) RF shield. (c) The EMI test stand of IPM.

The MCP readout cables are susceptible to electromagnetic noise. Therefore, all the IPM cables were enclosed in a Faraday cage, with small gaps filled using indium.

ISBN: 978-3-95450-249-3 ISSN: 2673-5350 doi: 10.18429/JACoW-IBIC2024-WEP18

In order to verify the electromagnetic compatibility of the RF shield and Faraday cage, tests were conducted using the Goubau Line. The Goubau Line comprises a field launcher and insulated wire, allowing the transmission of beam-like electromagnetic waves. One end of the G-Line was excited with a 2 kV, 2 ns signal at a repetition rate of 25 Hz, while the other end was terminated with a suitable high-power 50 Ω terminator. The experimental setup is depicted in Fig. 3 (c). A high-voltage pulsar with a set pulse width was employed to imitate the RCS beam. This setup is adequate for frequencies up to 500 MHz, meeting the requirements of up to 50 MHz of RCS beam. While a network analyzer can measure electromagnetic compatibility across the wider frequency spectrum, it was unsuitable due to the need for high power. Figure 4 displays the results of the SE experiment. Removing the top cover of the MCP resulted in a significant signal being induced on the anode strip. The induced signal was significantly reduced by fully closing the Faraday cage, achieving about −42 dB of SE.

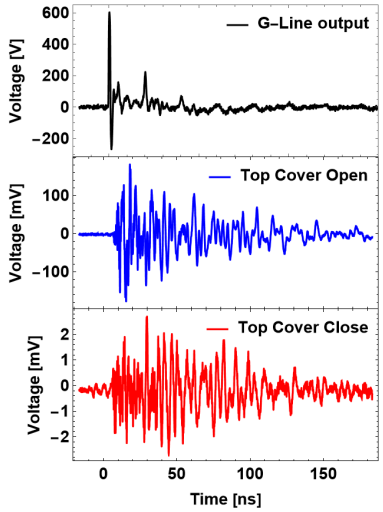


Figure 4: The EMI test results. When the top cover of the MCP was removed, a significant signal was induced on the anode strip. The induced signal was significantly reduced with a fully closed FC.

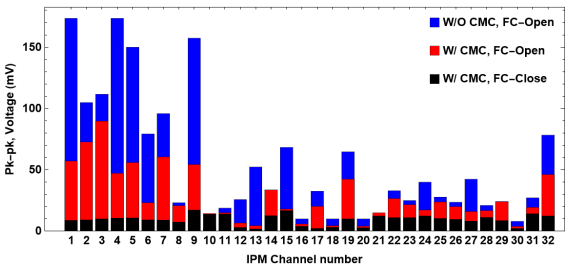


Figure 5: The beam-induced image current suppression with improved Faraday cage.

The improved IPM has been installed on the beamline. The bar chart in Fig. 5 displays the beam-induced image current on the anode strips of the MCP. Despite the improvements, we only achieved about -20 dB of SE. The target of −42 dB SE, as shown in the lab test, was not achieved. One potential reason could be the displacement of Faraday cage parts and indium filling during the MCP installation. Due to limited maintenance time, the SE test couldn't be performed again.

## *MCP Operation*

Two independent power supplies were utilized to provide high voltage to the MCP IN and OUT terminals. When high voltage is applied to the MCP IN terminal, strip current flows through the MCP, which cannot be sufficiently dissipated via the MCP OUT power supply, resulting in the inability to achieve the desired gain of the MCP. To address this issue, a pull-down resistor was incorporated into the MCP OUT power supply circuit. Figures 6 (a) and (b) illustrate the beam signal from one of the anode strips of the MCP without and with the appropriate pull-down resistors, respectively. The inclusion of the pull-down resistor enabled the desired MCP gain to be attained.

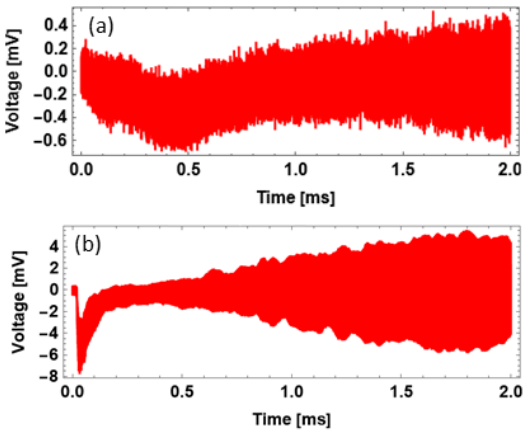


Figure 6: (a) The beam signal from one of the anode strip without pull-down resistor added to power supply circuit. (b) The beam signal with 1 MΩresistor added to MCP out power supply circuit.

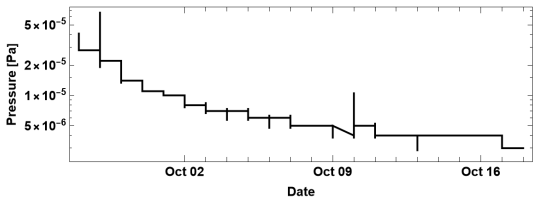


Figure 7: Vacuum pressure history data.

## *Vacuum Issues*

In the preceding sections, it was mentioned that in order to improve the SE, an RF shield and a sealed Faraday cage with indium were implemented. The Faraday cage only has a vacuum vent through the RF shield opening. The MCP, which is also located in the FC, requires a vacuum pressure

ISBN: 978-3-95450-249-3 ISSN: 2673-5350 doi: 10.18429/JACoW-IBIC2024-WEP18



of $10^{-4}$ Pa to operate. Initially, the desired vacuum pressure of $10^{-6}$ Pa couldn't be achieved due to the limited vacuum venting ports on the Faraday cage. It took nearly a month to reach the pressure of $1 \times 10^{-6}$ Pa. Figure 7 shows the history of the vacuum pressure data, which initially started at high levels due to gas leakage from the Faraday cage and eventually reached $10^{-6}$ Pa. To achieve a faster vacuum recovery, additional vacuum vents are necessary.

### *Analysis Techniques*

The beam-induced noise has been significantly reduced by -20 dB. However, the Faraday cage still exhibits imperfections, and noise is still noticeable. To tackle this issue, we collected data with the field cage of the IPM in both ON and OFF conditions while the MCP was ON in both cases. The data obtained in the field cage OFF condition was then subtracted from the field cage ON case. In Fig. 8, the IPM signal without background subtraction is displayed, where the noise is predominant. In contrast, Fig. 8 shows the IPM signal with background subtraction, resulting in the exclusion of the image current.

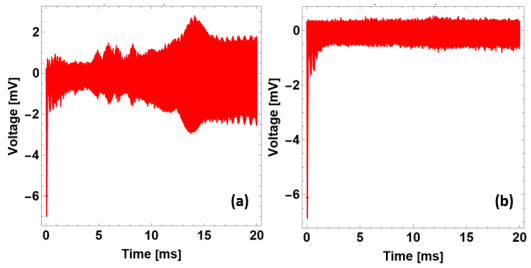


Figure 8: (a) The IPM signal without background subtraction. (b) The IPM signal with background subtraction. The image current can be excluded with background subtraction.

## BEAM PROFILE MEASUREMENT

The bunch-by-bunch horizontal beam profile of the RCS beam was successfully observed from the IPM. Figure 9 left shows the measured beam profile from IPM at 80 kW beam power, the horizontal axis is the position of anode strips and the vertical axis is the time. The beam profile can be observed only up to 200 μs due to MCP saturation. In order to confirm the MCP saturation, an experiment with the beam power of 8 kW was also carried out. Figure 9 right shows the horizontal beam profile of beam power 8 kW. In this case the signal can be seen for 1 msec. In order to observe the beam profile at the desired time interval of the acceleration cycle, the MCP saturation issue needs to be solved. The gated IPM [6] is currently under consideration to solve this issue.

## SUMMARY

An IPM prototype was designed for the CSNS RCS, and during beam commissioning, several challenges have been faced related to EMI, vacuum, and MCP power supply coupling. To address these issues, an RF shield was placed in front of the MCP and improved the Faraday cage with indium sealing, effectively reducing the EMI noise to -20 dB. Despite all of these mitigations, noise from the beam persisted. Therefore, a background subtraction technique has to be employed to mitigate this issue. In addition, an appropriate pull-down resistor is added to the MCP OUT power supply to ensure the gain of the MCP. We observed the bunch-by-bunch beam profile at 80 kW of beam power for approximately 200 μs, but noticed MCP signal saturation after 200 μs, resulting in reduced signal amplitude. To investigate this effect, experiments with varying beam power were conducted, allowing us to observe the beam signal for about 1 msec. The bunch-by-bunch horizontal beam profile was observed, and the gated IPM system with an improved MCP has been proposed for the CSNS RCS.

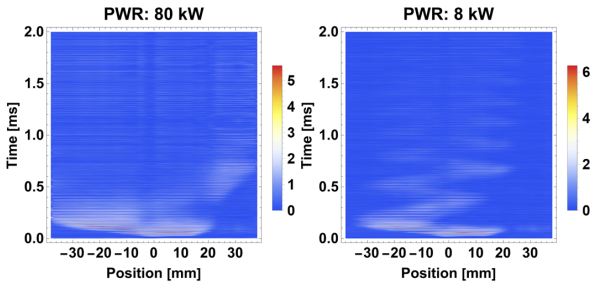


Figure 9: The bunch by bunch horizontal beam profile with different beam power.

## ACKNOWLEDGMENTS

We thanks Prof. Kenichihro Satou of J-PARC, James Storey, Jean Cenedl of CERN, and Dirk Bartkoski for the fruitful discussion.

## REFERENCES

[1] J. Wei, *et al.*, "China Spallation Neutron Source: Design, R & D and Outlook", *Nucl. Instrum. Methods Phys. Res., Sect. A*, vol. 600, no. 1, pp. 10-13, Feb. 2009, s doi:https://doi.org/10.1016/j.nima.2008.11.017

[2] W. Sheng, *et al.*, "Introduction to the overall physics design of CSNS accelerators", *Chinese Physics C*, vol. 33, no. s2, pp. 1-3, Jun. 2009, doi:10.1088/1674-1137/33/S2/001

[3] V. Dudnikov, " The intense proton beam accumulation in storage ring by charge-exchange injection method", Ph.D. Thesis, Novosibirsk INP, Novosibirsk, Russia, 1966.

[4] Hamamatsu Photonics, https://www.hamamatsu.com/us/en.html

[5] C. R. Paul, "Introduction to Electromagnetic Compatibility", *John Wiley & Sons Inc.*, New Jersey, USA, Sep. 2005. doi:10.1002/0471758159

[6] K. Satou, S. Igarashi, and Y. Sato, "Merits of Pulse Mode Operation of Residual Gas Ionization Profile Monitor for J-PARC Main Ring", in *Proc. IBIC'22*, Kraków, Poland, Sep. 2022, pp. 434–437. doi:10.18429/JACoW-IBIC2022-WEP21